Ocean Systems Engineering, *Vol. 14, No. 4 (2024) 383-404*
https://doi.org/10.12989/ose.2024.14.4.383

Numerical study on thermal buckling analysis of different multilayer offshore pipelines

Balan Raju and Vadivuchezhian Kaliveeran*

Department of Water Resources and Ocean Engineering, National Institute of Technology Karnataka India

(Received March 8, 2024, Revised May 20, 2024, Accepted May 30, 2024)

Abstract. Thermal buckling is one of the major problems in offshore pipelines, which affects the structural integrity of the pipeline since it operates under extreme temperatures and high-pressure conditions. The temperature variations across the pipeline's radius govern the critical buckling temperature, arising from heat transfer, especially the natural convection between the working fluid medium and the surrounding fluid medium. In the present study, the finite element tool ANSYS is selected to execute a coupled steady-state thermal and linear eigenvalue buckling analysis on four different types of offshore pipelines: equivalent single-walled pipeline, lined pipeline, sandwich pipeline, and pipe-in-pipe system. The critical buckling temperature of these pipelines is evaluated under subsea and buried conditions, and in comparison, to that of an equivalent single-walled pipeline. The temperature variation and Von Mises stress across the radius of the pipelines are analyzed. The results show that the addition of insulation materials to the pipelines has a significant impact on their critical buckling temperature. The pipe-in-pipe system shows a higher critical buckling temperature than all the other pipelines, exhibiting a significant rise in temperature and outperforming the equivalent single-walled pipeline by 116% and the sandwich pipeline by 34%. Furthermore, the lined pipe's critical bucking temperature is almost the same as that of the equivalent single-walled pipeline.

Keywords: critical buckling temperature; natural convection; offshore pipelines; steady-state heat transfer; thermal buckling

1. Introduction

Offshore pipeline transportation has emerged as one of the most dependable, safest, and most practical ways to move petroleum products and natural gas from oil wells to processing stations at a low cost compared to other transportation methods in recent years (Li *et al.* 2024, Abyanifor and Bahaari 2021, Vishnuvardhan *et al.* 2023). The scarcity and demand for offshore crude oil and natural gas have increased continuously in recent years (Moghaddam *et al.* 2015). As a result, it has become essential for offshore industries to study oil exploration fields from deep-water to ultra-deep-water conditions (Guo *et al.* 2016). In these conditions, operating temperatures and pressures can exceed 150°C and 70 MPa, respectively (Vishnuvardhan *et al.* 2023, Vazouras *et al.* 2021, Karar *et al.* 2021). The pressure variation and temperature difference are the two main factors that influence the axial force in the pipeline (Guo *et al.* 2013).

*Corresponding author, Associate Professor, E-mail: vadivuchezhian_k@nitk.edu.in

http://www.techno-press.org/?journal=ose&subpage=7 ISSN: 2093-6702 (Print), 2093-677X (Online)

In these high-pressure (HP) and high-temperature (HT) working environments, offshore pipelines are easily susceptible to thermal buckling, whether the pipelines are deployed or buried on the seafloor.

However, pipeline elongation is limited due to seabed friction (Zhang and Duan 2015, Hobbs 1984) and pipeline end conditions (Hobbs 1984). When the pipeline reaches its critical buckling load, the axial compressive stresses are alleviated through buckling (Hobbs 1984, Wang *et al.* 2021, Wang *et al.* 2024). Generally, global thermal buckling in offshore pipelines can be classified into two forms, namely lateral buckling and vertical buckling. Lateral buckling predominantly takes place in deep water conditions where the pipelines are installed on the seafloor. In this installation, the pipelines can freely move in the lateral direction due to insufficient resistance when exposed to extreme environmental conditions; whereas, vertical buckling occurs in situations where the pipelines are buried or trenched (Subedi *et al.* 2024, Ismail *et al.* 2021, Rajeev and Robert 2017). The buckling results in uncontrollable deformation, pipeline rupture, leakage, local buckling, and fatigue (Cai *et al.* 2023). Additionally, it affects the marine ecosystem, marine environment, oil/gas reserves, and project costs (Subedi *et al.* 2024, Cai and Grognec 2022, Wang *et al.* 2023).

The majority of the research work on offshore thermal buckling analysis is predicated on the premise that the temperature deviation of petroleum products from the environmental conditions, i.e., surrounding seawater temperature, is considered constant (Wang *et al.* 2021). However, only a few research studies have addressed steady-state heat transfer in global thermal buckling (Wang *et al.* 2017). Heat transfer analysis is one of the main thermal analyses for offshore pipelines, used to obtain the temperature profile across their thickness with suitable boundary conditions. Typically, when conducting heat transfer analysis for offshore pipelines, both steady-state and transient states are taken into account. The transient analysis is particularly useful in determining the temperature changes that occur during shutdown (Cheng *et al.* 2010) and start-up operations (Wang *et al.* 2019).

In real-time conditions, a temperature gradient occurs between oil flow and surrounding seawater. Consequently, the transfer of heat from crude oil to the surrounding environment occurs predominantly through conduction and convection (Guo 2005). As the crude oil travels through the pipeline, its temperature undergoes a continuous reduction due to heat losses resulting from conduction and convection modes of heat transfer (Barletta *et al.* 2008). The temperature inside the pipeline falls to the Wax Appearance Temperature (WAT) as a result of heat dissipation to the outside atmosphere, which initiates the formation of wax in the pipelines (Escobedo *et al.* 2005, Bell *et al.* 2021). The formed waxes and hydrates have an impact on pipeline flow assurance by restricting the flow passage and increasing the pipeline's power input. The occurrences of paraffin and hydrates in the pipelines are avoided by using proper insulation methods (Escobedo *et al.* 2005). In HP/HT conditions, the offshore pipelines are insulated with various polymeric materials to avoid wax and hydrate formation. The heat losses of the offshore pipelines are controlled by using two different types of techniques: passive control and active heating control (Bell *et al.* 2021). In the passive control method, the heat losses are prevented by adding insulation layers, liners, and various materials to the offshore pipelines. Another passive control method involves burying the offshore pipeline under the seafloor. In the active heating approach, electrical and hot fluid heating methods are used to control the heat losses. The majority of research, encompassing theoretical, computational, and experimental works, on global thermal buckling of offshore pipelines has been focused on single-walled pipelines (Li *et al.* 2021, Mondal and Dhar 2017,

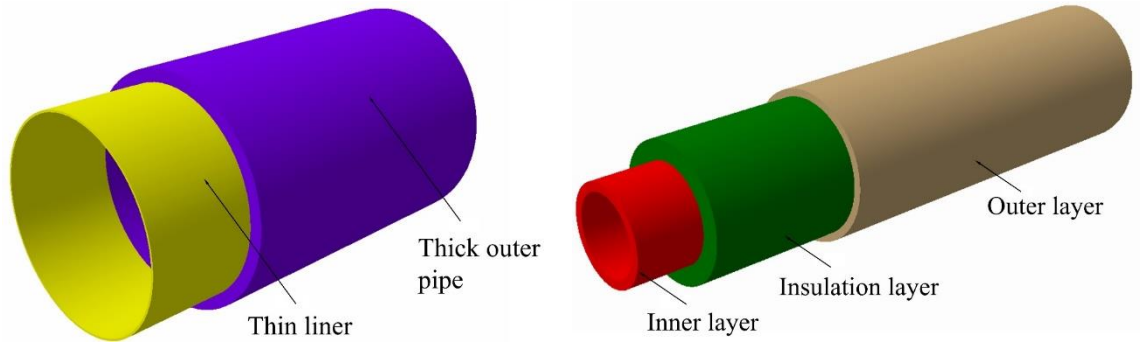

(a) Lined pipeline (b) Compliant PIP

Fig. 1 Types of pipeline system

Wang *et al.*2015).

Two steel tubes are positioned in a concentric manner to form a pipe-in-pipe system (PIP) (Wang *et al.* 2022, Castello and Estefen 2008). The annular gap between the inside and outside of the PIP systems is either vacant or occupied with insulation materials (Kyriakides 2002). An internal pipe within the PIP system carries crude oil, while the external pipe, known as the carrier, secures the insulation material from environmental conditions (Zhang *et al.* 2016). Conversely, a sandwich pipeline is a composite or multilayer pipeline made up of multiple material layers that are adhered together and function as a single-layer pipeline (Bhardwaj *et al.* 022). The core material in the sandwich pipelines is involved in both thermal and structural applications, whereas, in the PIP systems, the core material is not involved in any load-carrying structural applications (Yang *et al.* 2024, Castello and Estefen 2008). A lined pipe, also known as a "bi-material pipe," is made up of a thick outer pipe and a thin-walled inner pipe that are joined together using a specific production method. The lined pipeline's inner pipe, or liner, is a thin layer of generally 2-3 mm thick corrosion-resistant alloy material, as opposed to the lined pipeline's outer pipe, which is constructed of low-carbon steel (Wang and Soares 2022, Yuan and Kyriakides 2014). Fig. 1 depicts a schematic illustration of the lined pipe and compliant PIP.

The buckling phenomenon in sandwich pipes and PIP systems exhibits a significantly higher level of intricacy when compared to an equivalent single-walled pipeline. This is due to the interaction among the inner, outer, and insulating layers, as well as the different coefficients of thermal expansion between the insulation layer and the pipeline materials (Zechao *et al.* 2020). The present study aims to examine how temperature fluctuations across the radius influence the critical buckling temperature in multilayer offshore pipelines using thermal buckling analysis. The present numerical analysis will focus on four different types of pipelines. These include the equivalent single-walled pipeline, PIP system, sandwich pipeline, and lined pipeline. The temperature variations occurring on these pipelines are computed by utilizing ANSYS to conduct steady-state heat transfer analysis. Further, the obtained temperature variation from the heat transfer analysis is incorporated into the linear eigenvalue buckling analysis. The computed critical buckling temperature associated with these pipelines is contrasted with the critical buckling temperature of an equivalent single-walled pipeline. This numerical analysis focuses solely on the linear eigenvalue buckling analysis of the pipelines. For the study of the effect of embedment depth on critical buckling temperature under buried conditions, three different embedment depths,

such as 500 mm, 750 mm, and 1000 mm, were considered in the numerical analysis of a single-walled pipeline.

2. Problem formulation and material properties

2.1 Problem formulation

The temperature variation over the pipelines' cross-sectional area is obtained by using time-independent heat transfer analysis. For a three-dimensional cylindrical coordinate system, the governing differential equation for heat conduction is as follows (Holman 2010)

$$\frac{\partial^2 T}{\partial r^2}+\frac{1}{r}\frac{\partial T}{\partial r}+\frac{1}{r^2}\frac{\partial^2 T}{\partial \varphi^2}+\frac{\partial^2 T}{\partial z^2}+\frac{q_{gen}}{k}=\frac{1}{\alpha}\frac{\partial T}{\partial \tau} \tag{1}$$

where k represents the thermal conductivity of pipeline material, W/m°C; q_{gen} denotes the heat generation, W/m^3; α implies the thermal diffusivity of the material, m^2/s. For the current numerical analysis, the following presumptions are made: The temperature variation across the pipeline is time-independent (i.e., steady-state heat transfer) and varies only across the pipeline's radius. In this context, the temperature along the pipeline remains consistent throughout its length, and its impact on the properties of the pipeline materials is not accounted for in this analysis. Furthermore, internal heat generation is disregarded. Under this axisymmetric condition, the pipeline's temperature distribution is only a function of radius. Consequently, the heat transfer equation for 3D cylindrical coordinates can be reduced to the following equation

$$\frac{d^2 T}{dr^2}+\frac{1}{r}\frac{dT}{dr}=0 \tag{2}$$

The above equation yields the following result

$$T(r)=C\ln r+D \tag{3}$$

where the *C* and *D* are integration constants that are determined by using the mixed boundary conditions.

The pipeline's internal and external surfaces are subjected to a mixed boundary condition, also known as a convective boundary condition, which can be defined as follows

$$-k\frac{dT}{dr}=h_{in}(T-T_{\infty 1}) \text{ at inner radius } (r=r_{in}) \tag{4}$$

$$-k\frac{dT}{dr}=h_{ex}(T-T_{\infty 2}) \text{ at outer radius } (r=r_{ex}) \tag{5}$$

where $T_{\infty 1}$ and $T_{\infty 2}$ represent the petroleum product and the seawater temperatures, respectively, °C; h_{in} and h_{ex} denote the convection heat transfer coefficient of the internal and external surface of the pipeline, W/m^2 °C. The temperature variation across the radius of the equivalent single-walled pipeline is ascertained through the substitution of the mixed boundary conditions in Eq. (3). The temperature variation is given by Eq. (6)

$$T(r)=\frac{1}{\frac{k}{r_{in}h_{in}}+\ln\frac{r_{ex}}{r_{in}}+\frac{k}{r_{ex}h_{ex}}}\left\{[T_{ex}-T_{in}]\ln r+\left[T_{in}\ln r_{ex}-T_{ex}\ln r_{in}+\frac{k}{r_{ex}h_{ex}}T_{in}+\frac{k}{r_{in}h_{in}}T_{ex}\right]\right\} \tag{6}$$

Table 1 Fluid properties of crude oil and seawater (Castello and Estefen 2008)

Parameter	Crude oil	Sea water
Temperature, T, °C	80	4
Density, ρ, (kg/m^3)	800	1025
Dynamic viscosity, μ, (Ns/m^2)	0.06712	0.00175
Thermal conductivity, k, (W/m °C)	0.14	0.57
Specific heat capacity, c, (kJ/kg °C)	2.7	4.217

Table 2 Geometrical and material properties of pipelines (Wang *et al.* 2017, Castello and Estefen 2008)

Parameter	Outer Pipe	Inner pipe	Liner	Polypropylene	Polyurethane
Diameter (mm)	152	98	-	-	-
Thickness (mm)	7.6	9.2	3	19.4	19.4
Density, ρ, (kg/m^3)	7800	7800	7800	893	700
Young's Modulus, E, (GPa)	206	206	191	5.06	0.067
Coefficient of thermal expansion, α, (1/°C)	1.17 x 10^{-5}	1.17 x 10^{-5}	1.7 x 10^{-5}	9.92 x 10^{-5}	0.0023 x 10^{-5}
Thermal conductivity, k, (W/m °C)	55.6	55.6	16.3	0.0415	0.03

In a similar manner, we can determine the temperature distribution across the radius of the lined, pipe-in-pipe, and sandwich pipelines.

The fluid properties of seawater and crude oil are tabulated in Table 1. The sandwich and pipe-in-pipe systems employ the API 5L-X65-grade steel material in both the inner and outer pipes, as well as for the outer layer of the lined pipeline. The pipeline's material properties are listed in Table 2.

The insulation layer in the sandwich pipeline is made of polypropylene, whereas polyurethane foam is used for the insulation portion in the PIP system. The corrosion-resistant alloy (CRA) SS316L is used as the liner material for the lined pipe. Buckling is characterized by localization, indicating that it happens only in a specific section of the pipeline and does not affect the entire length (Wang et al., 2017). Therefore, the current numerical analysis involves evaluating pipelines with a length of 5 m for both steady thermal and buckling analyses. The diameter of the equivalent single-walled pipeline is 152 mm, while its thickness is 36.2 mm. Generally, the pipeline's inside and outside walls are in direct contact with a fluid medium, i.e., crude oil and seawater. As a result, convection heat transfer takes place in the pipeline. The inner and outer convection heat transfer coefficients are calculated based on fluid properties, the pipeline's diameter, and the velocities of the crude oil and seawater. In this numerical analysis, the flow velocity of crude oil/fluid is 0.1 m/s, whereas the flow velocity of seawater is 1 m/s. For the buried pipeline analysis, clay is considered for this numerical analysis. The mechanical properties of the clay were represented using the Mohr-Coulomb criteria, defined by parameters such as cohesion of 20 kPa, Young's modulus of 25 MPa, Poission's ratio of 0.49, and coefficient of friction of 0.4.

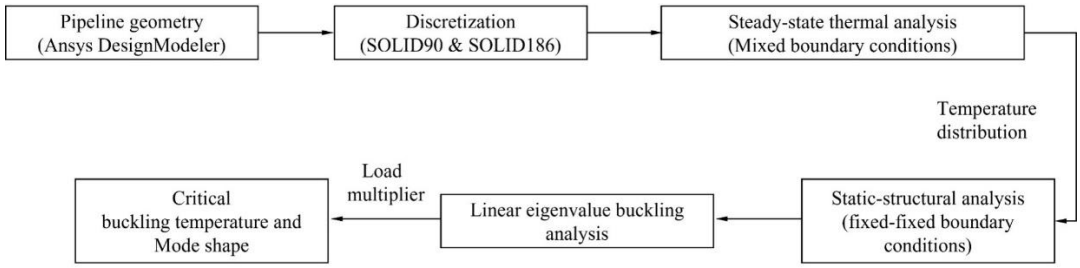

Fig. 2 Thermal buckling simulation process

2.2 Finite element analysis

The procedure involved in the coupled study of steady-state heat transfer to linear eigenvalue buckling process is illustrated in Fig. 2. Three main steps are involved in the present numerical analysis. In the first step, a steady-state heat transfer analysis is performed using the input values of internal and external heat transfer coefficients. As a result, the temperature distribution is obtained across the cross-section of the pipeline. In the next step, the obtained temperature load is incorporated into the static structural analysis with fixed-fixed boundary conditions which induce stresses in the pipeline. Finally, the findings obtained from the static structural analysis are employed as the initial conditions for subsequent linear eigenvalue buckling analysis.

ANSYS DesignModeler was used to create 3D geometric models of the single-walled, lined, sandwich, and PIP systems. Fig. 3 provides a front view of all the pipeline models. In this numerical analysis, we have not considered the centralizer ring for the PIP system. Typically, this ring is utilized to keep the pipes concentrically aligned. Instead, a compliant PIP system with a polyurethane insulation layer is used.

The pipeline models are discretized using 3D solid elements, such as SOLID90 and SOLID186, to compute the thermal and mechanical responses of the structure. While performing static structural analysis, the SOLID90 element is substituted by the SOLID186 element. The SOLID90 element is a higher-order 20-node thermal element having one degree of freedom (DOF) per node, i.e., temperature. The SOLID186 is a higher-order three-dimensional hexahedral, 20-node element that contains three DOF per node, i.e., displacement in x, y, and z directions. It is very well suited for simulating situations that involve large strains, large displacements, plastic deformation, stress stiffening, and hyperelasticity (ANSYS, 2019).

A Bonded type of contact is established, connecting the polyurethane and polypropylene insulating layers with the API 5L-X65 grade steel pipes in PIP and sandwich pipelines. The bonded contact prevents the pipeline layers from sliding. The 3D numerical model of the subsea and buried pipeline is illustrated in Fig. 4.

The contact between the layers is modeled by the ANSYS contact element CONTA174 and the corresponding target element TARGE170. These are frictionless contact elements used for 3D structural and coupled field contact analysis. A mesh convergence analysis is conducted for all pipelines to compute the accurate critical buckling temperature since the numerical analysis results may vary depending on the mesh sizes. The obtained thermal load from the steady-state thermal analysis is given to the static structural analysis, where the fixed-fixed boundary conditions are assigned to the two extreme faces of the pipeline through fixed support in ANSYS. Fig. 5 shows the element configuration of the SOLID186.

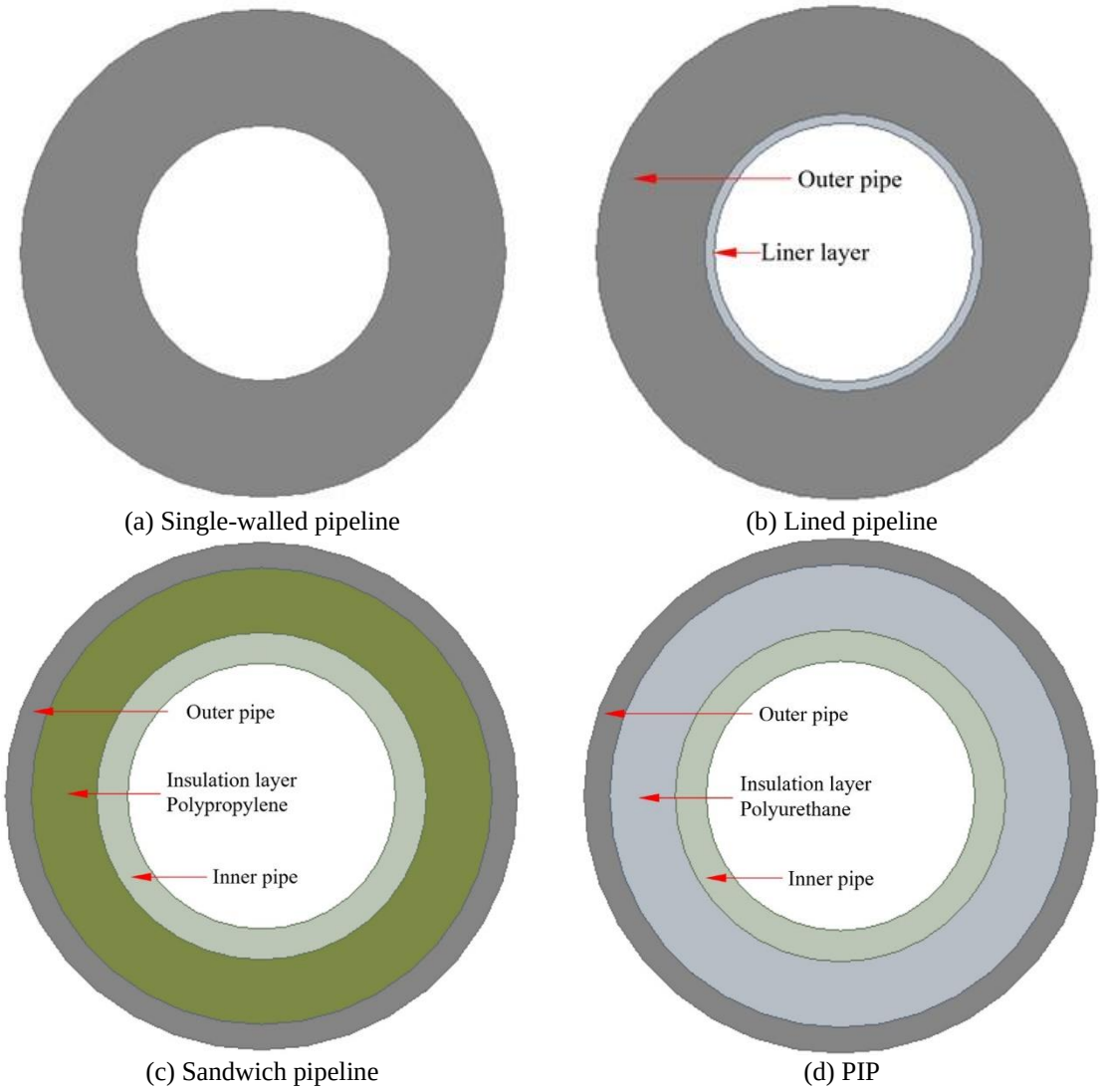

(a) Single-walled pipeline (b) Lined pipeline

(c) Sandwich pipeline (d) PIP

Fig. 3 Front view of the offshore pipeline models

The pipelines are subjected to fixed boundary conditions at z = 0 m and z = 5 m, illustrated in Fig. 6. The displacement and rotation DOF at either extremity of the pipelines are zero in the fixed-fixed boundary condition. These boundary conditions arrest rotational and translational movement in all directions of the pipeline.

2.3 Linear eigenvalue buckling analysis

The general governing equation for linear eigenvalue buckling is given as follows.

$$\left([K_e] + \lambda_i [K_g]\right)\{\psi_i\} = 0 \tag{7}$$

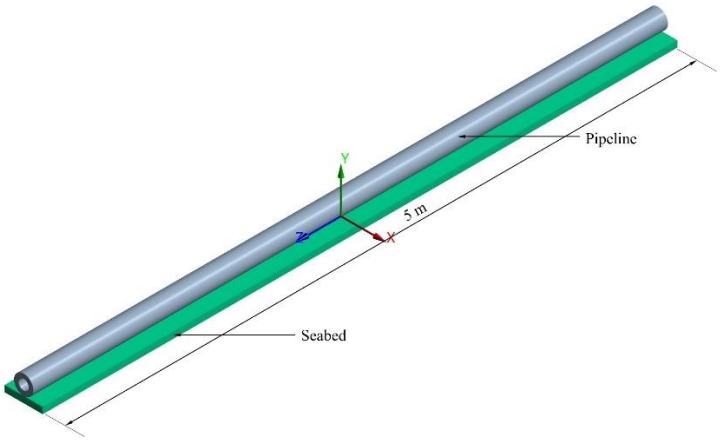

(a) Subsea pipeline

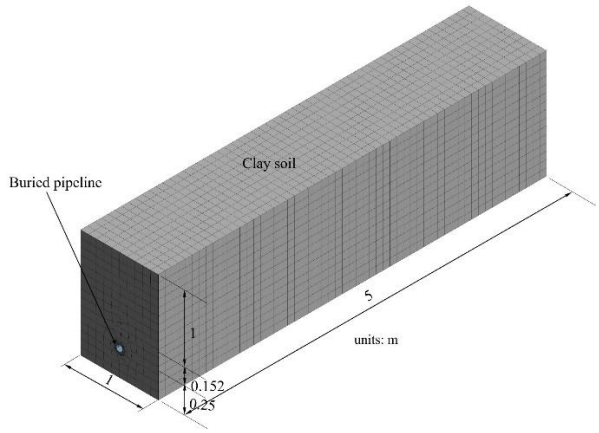

(b) Buried pipeline

Fig. 4 3D Numerical model of a buried and subsea pipelines

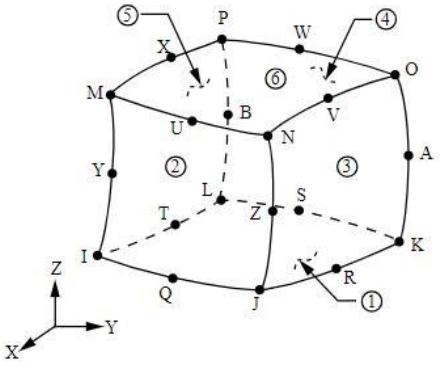

Fig. 5 SOLID186 element configuration (ANSYS, 2019)

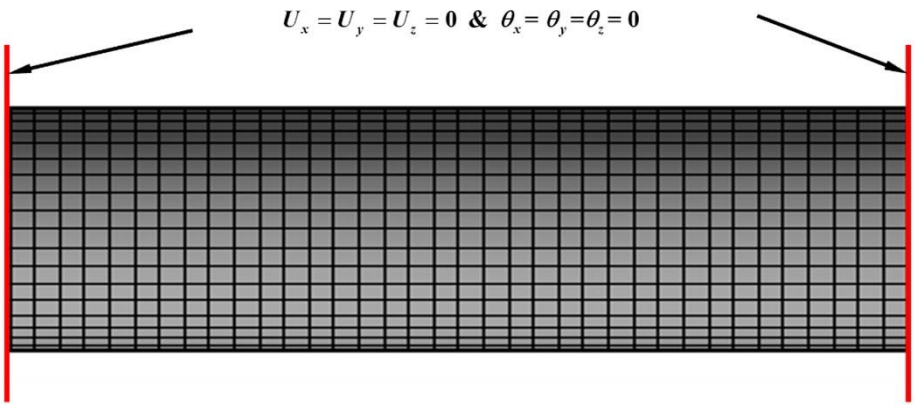

Fig. 6 Fixed-Fixed boundary condition

here K_e represents the elastic stiffness matrix, K_g denotes the geometric stiffness matrix of the structural member, λ_i and ψ_i represent the eigenvalue and corresponding eigenvector, respectively.

The outcomes of the stress analysis are fed into eigenvalue buckling analysis, which yields the load multiplication factor and buckled shape. The lowest eigenvalue and the maximum temperature of the steady-state thermal analysis are used to figure out the critical buckling temperature of the pipelines (Liu 2011, Chen *et al.* 2019).

3. Results and discussion

3.1 Temperature variation

Fig. 7 gives the temperature distribution of the pipelines, including equivalent single-walled, lined, sandwich, and PIP systems. From the steady-state thermal analysis, it can be observed that the maximum temperature of the single-walled, lined, sandwich pipeline, and PIP are 4.77°C, 4.83°C, 55.23°C, and 60.3°C, respectively.

Furthermore, the steady-state thermal analysis revealed that the highest temperature occurs at the internal surface of the aforementioned pipelines. The temperature variation through the pipeline radius is shown in Fig. 8. In the single-walled and lined pipelines, the temperature variation across the radius decreases from internal to external surfaces. The temperature on the internal surface of single-walled and lined pipelines closely approaches the surrounding seawater temperature due to the high convective heat transfer coefficient on their external surface. Therefore, insulation is necessary to inhibit the occurrence of paraffin and hydrate formation within the pipeline. The lined pipeline's temperature gradient is significantly higher on the inner liner layer compared to the outer pipe. The temperature variations across the insulation layers in the sandwich and PIP pipelines decrease linearly with increasing insulation layer radius.

The temperature variation remains nearly uniform for both the sandwich's and the PIP system's inner and outer pipes due to their higher heat conductivity compared to the insulation layer.

Moreover, there is a higher temperature gradient in the insulating layers compared to the inner and outer pipes in both sandwich and PIP systems. Particularly, the PIP system exhibits a slightly higher thermal gradient than the sandwich pipe system. The insulation material in the sandwich

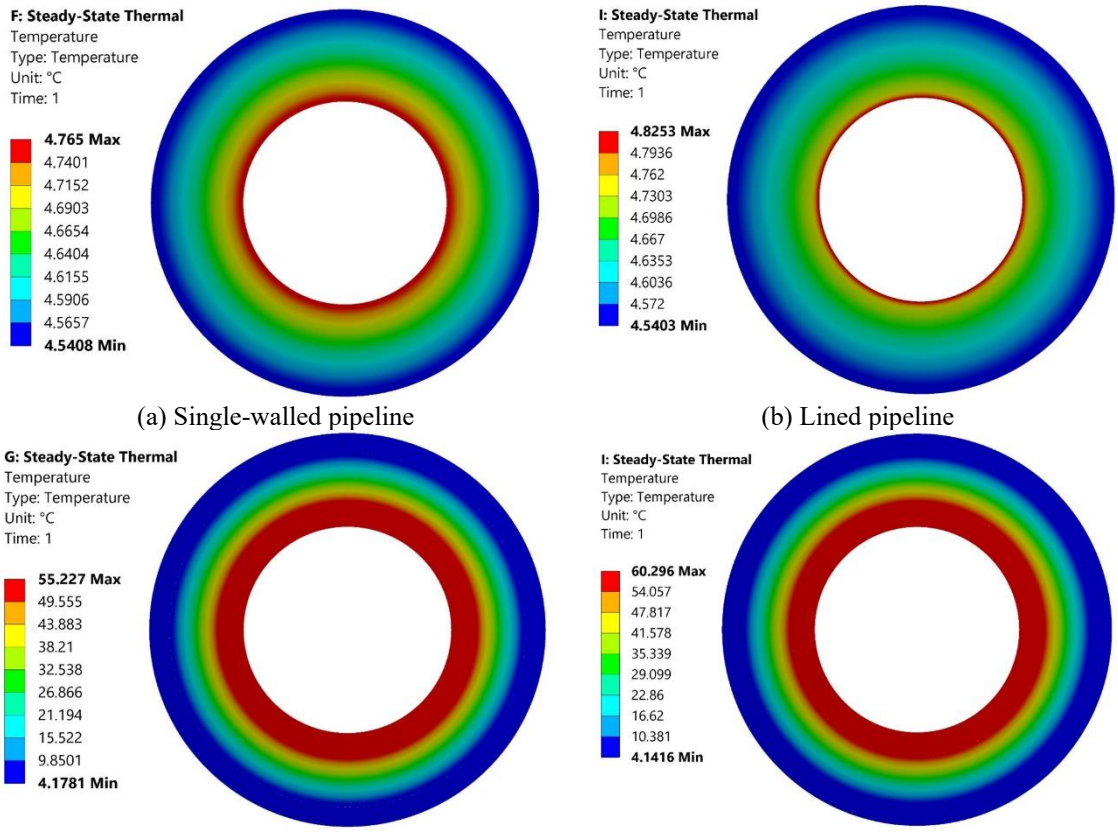

(a) Single-walled pipeline (b) Lined pipeline

(c) Sandwich pipeline (d) Pipe-in-pipe system

Fig. 7 Temperature variations of various pipeline types

and PIP system effectively minimizes the transfer of heat between the outer and inner surfaces, leading to a drastic change in the temperature variation across the radius of the pipeline.

3.2 Von Mises stress variation

The changes in Von Mises stresses across the radius of the pipelines are depicted in Fig. 9. The stress developed in the single-walled pipeline decreases along the radius due to the proportional relationship between stress and temperature change, as shown in Fig. 9(a). When it comes to the lined pipeline, as shown in Fig. 9(b), the sudden temperature drop at the liner radius causes abrupt stress variation along the radius of the lined pipeline up to the liner material. Within a 3 mm inner radius of the lined pipe, stress decreases rapidly compared to the rest of the pipe radius.

The insulation layers, such as polypropylene and polyurethane, experience significantly lower stresses than the pipeline's inner and outer pipes, primarily attributed to their very low elastic modulus as shown in Figs. 9(c) and 9(d).

The stress variation along the radius of the PIP system and sandwich pipeline, which consists of an outer steel pipe, an inner steel pipe, and an insulation layer (i.e., polypropylene and polyurethane), depends on several factors. These factors include the temperature gradient across the pipeline, the

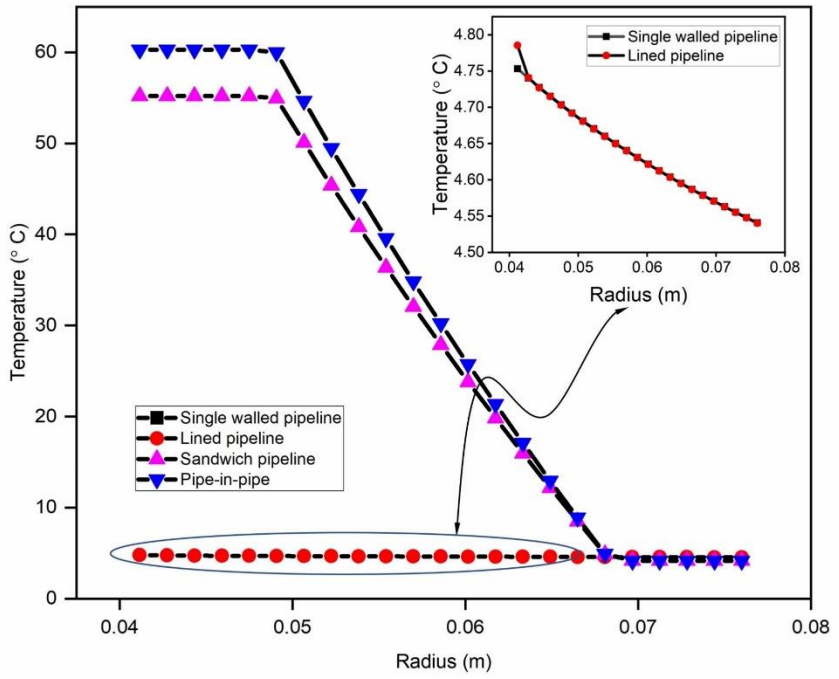

Fig. 8 Temperature changes along a radius of various pipelines

material's Young's modulus, and their respective thermal expansion coefficients. The aforementioned factors also cause the pipe's flexural stress, which varies with the pipeline's radial distance.

Since the outer surface of the pipeline is situated farther from its neutral axis. As a result, the outer pipe experienced higher flexural stress than the inner pipe and insulation layer. The sandwich pipeline's inner temperature is 55.23°C, which is greater than the temperature of the outer pipe at 4.18°C. The inner pipe and polypropylene layer experience higher elongation than the outer pipe due to the proportional relationship between temperature and the coefficient of thermal expansion with elongation. Consequently, the inner pipe experiences compressive stress, which causes the outer pipe to buckle sideways in the pipeline. In addition to the temperature changes, the pipeline's materials Poisson's ratio can also affect the stress variations in the pipeline. All of these elements bring about higher stress in the outer pipe of the sandwich pipeline, while the insulation layer experiences lower stress.

When the pipeline's temperature changes, the materials expand or contract due to their coefficient of thermal expansion. If the linear thermal expansion coefficients of the materials are different, then the expansion or contraction of one layer may cause stresses in the adjacent layers. The stress gradients in the lined, sandwich, and pipe-in-pipe pipelines are typically highest at the layer interfaces or boundaries due to sudden temperature gradients between the layers. In the pipe-in-pipe system, the inner pipe experiences higher stress as a result of the elevated temperature distribution, high modulus elasticity of the inner pipe material, and mainly the low coefficient of thermal expansion of the polyurethane insulation layer. In contrast, the polyurethane insulation layer experiences significantly lower stress because of its low thermal expansion coefficient and low modulus of elasticity.

Compared with the inner pipe as well as the polyurethane layer, the outer pipe contracts significantly in the PIP due to the temperature decrease from 60.3°C to 4.14°C. This leads to the inner pipe

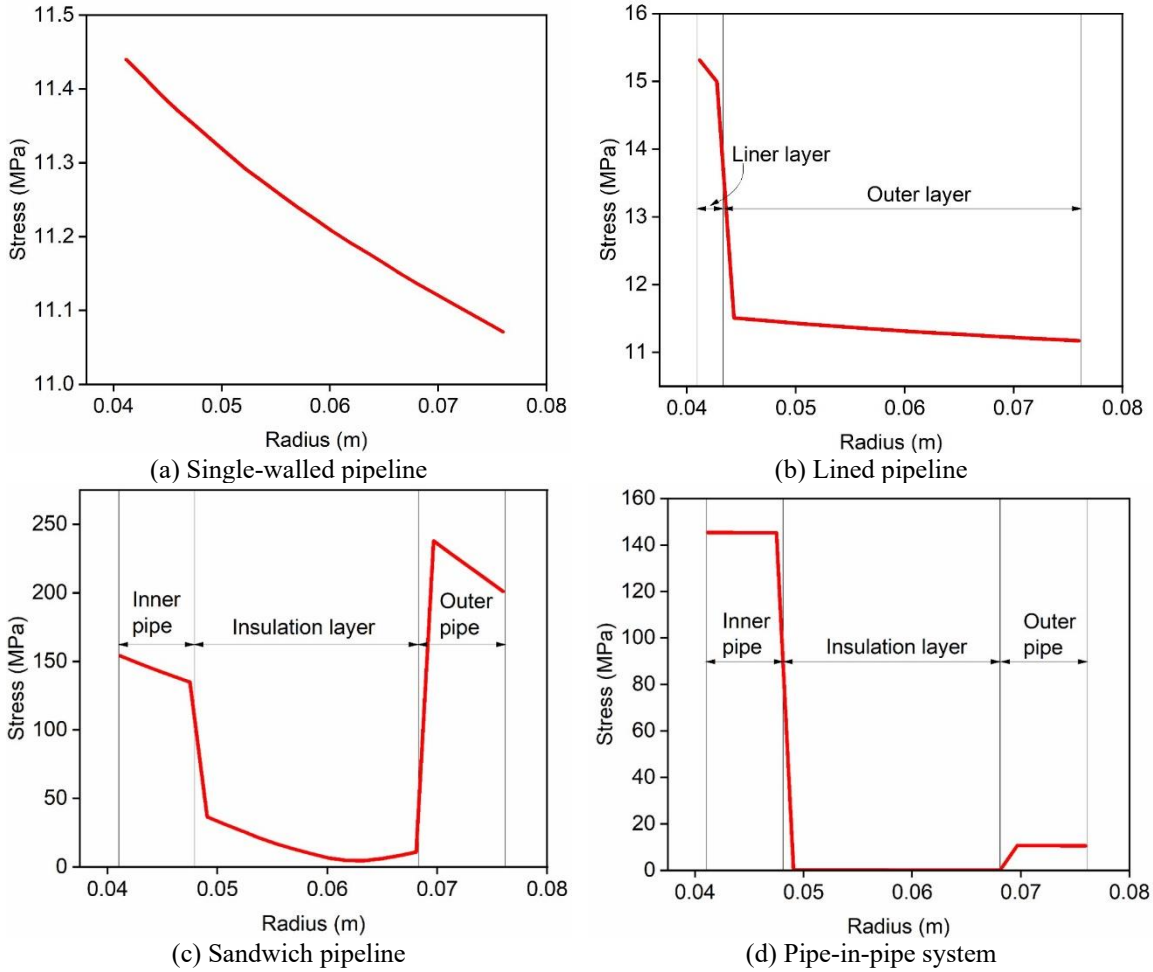

(a) Single-walled pipeline (b) Lined pipeline

(c) Sandwich pipeline (d) Pipe-in-pipe system

Fig. 9 Von Mises stress variations of pipelines

experiencing compressive stress, while the outer pipe undergoes tensile stress. However, because of its significantly lower elastic modulus than that of steel, the insulation layer has little impact on the overall stress distribution. Thus, the inner pipe of the PIP is subjected to more stress than the outer pipe. The static structural analysis revealed that the stress experienced by the sandwich pipeline exceeded that of the PIP. The insulating material in the sandwich pipeline thereby gives the pipe both insulation and structural strength.

3.3 Critical buckling temperature

The total deformation, i.e., normalized deformation, of the aforementioned pipelines is shown in Fig. 10.

The load multiplication factor for all the pipelines is greater than 1, indicating that the pipelines are safe and have not buckled under the given loading and boundary conditions. Fig. 11 illustrates the critical buckling temperature for various pipeline types.

The steady-state temperature distribution across the pipeline's cross-section plays a major role in computing its critical buckling temperature. The critical buckling temperature obtained from the eigenvalue buckling analysis depends on the maximum nodal temperature ($T_{\text{max. nodal}}$), which is determined from the steady-state heat transfer analysis of the pipelines and is given by the following expression (Liu 2011, Chen *et al.* 2019).

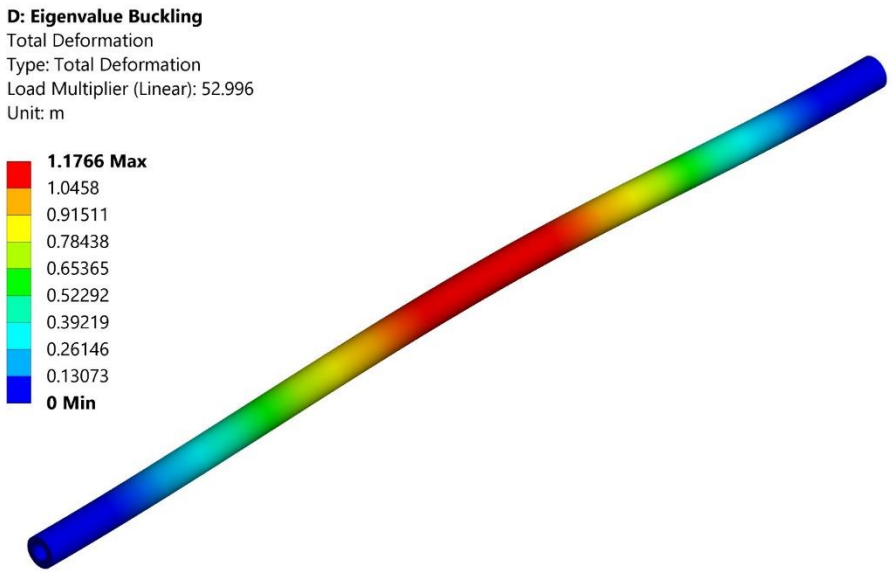

(a) Single-walled pipeline

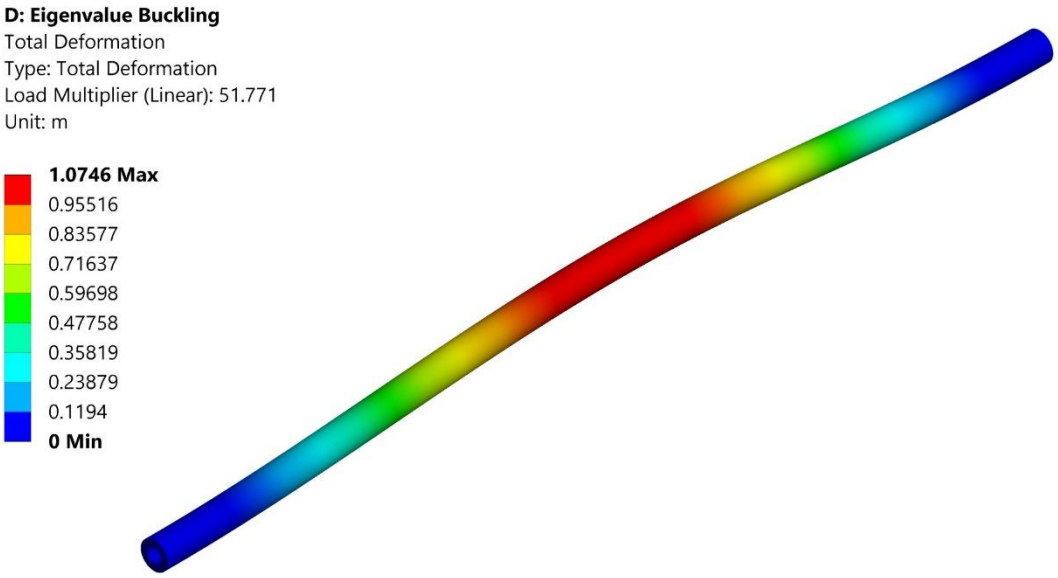

(b) Lined pipeline

Fig. 10 Total deformation of various pipelines

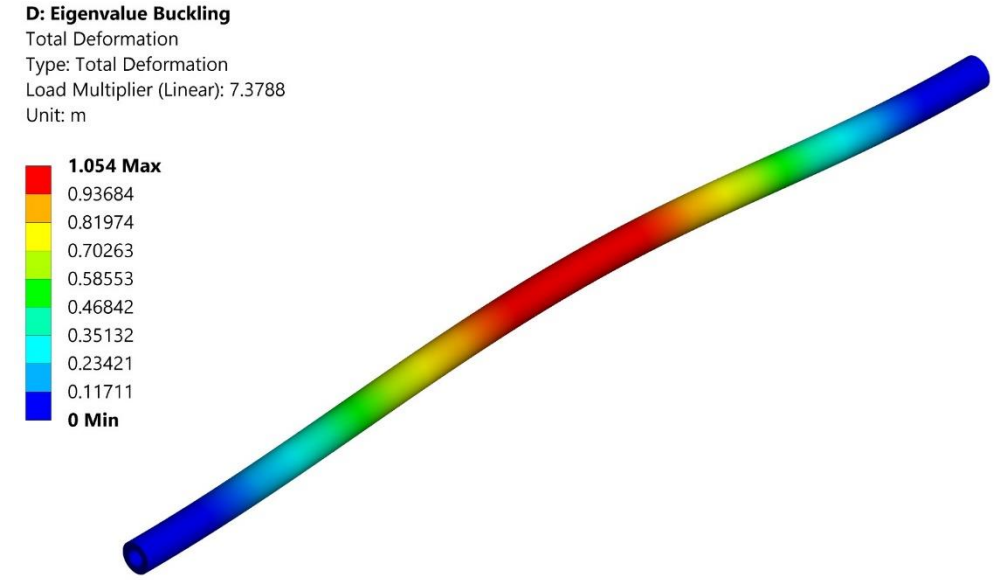

(c) Sandwich pipeline

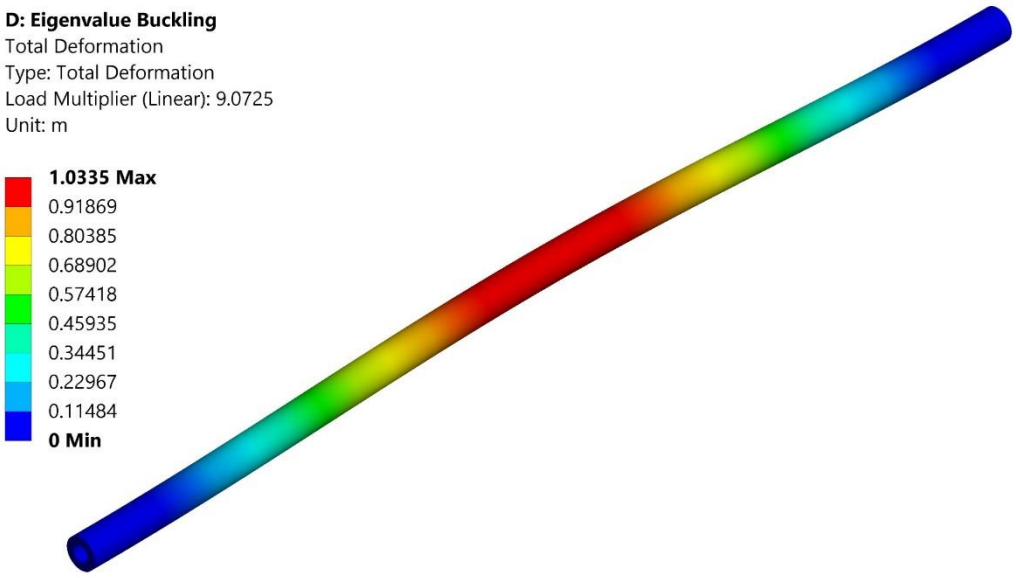

(d) Pipe-in-pipe system

Fig. 10 Continued-

$$(\Delta T)_{cri} = (T_{max.\ nodal})(\text{Load multiplier}) \tag{8}$$

For the single-walled pipeline, the maximum temperature obtained from the steady-state thermal analysis is 4.77°C, which is, moreover, uniform across the radius of the pipeline and is approximately equal to the outer temperature. Therefore, the critical buckling temperature computed from the numerical analysis is 252.8°C. Similarly, this behavior is also observed in the

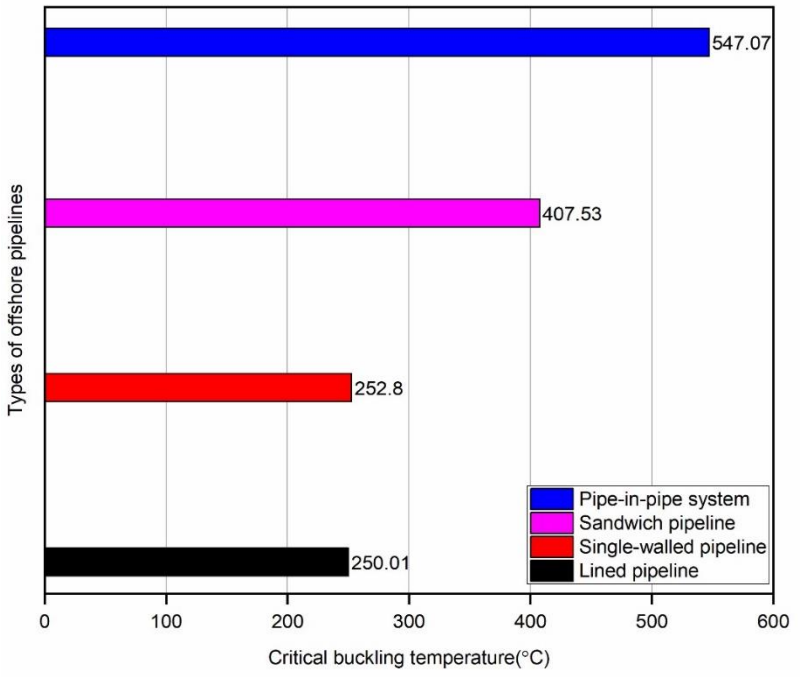

Fig. 11 Critical buckling temperature for various offshore pipelines

lined pipelines, where the temperature variation from the inner to outer pipes is very small, ranging from 4.5°C to 4.8°C. Consequently, the critical buckling temperature of the lined pipeline is 250.05°C. The addition of a 3 mm liner, made of a corrosion-resistant alloy, to the single-walled pipeline (i.e., lined pipeline) had no impact on the critical buckling temperature (250.05°C). The thermal buckling mechanism in PIP and sandwich pipelines is more complex than in single-walled pipelines due to the interactions among the inner, core, and outer pipes. It is evident from Fig. 8 that the temperature distribution across the thickness of the pipeline is significantly larger for sandwich and PIP systems compared to single-walled and liner pipelines. This directly affects the critical buckling temperature of the PIP and sandwich pipelines. Specifically, the temperature variation in the insulation layer can greatly affect the critical buckling temperature of the pipelines. As a result, the axial compressive forces differ for each pipeline due to the presence of liner and core layers, such as polyethylene and polyurethane, compared to a single-walled pipeline. The maximum nodal temperatures obtained from the heat transfer analysis for the sandwich and PIP systems are 55.23°C and 60.3°C, respectively. Therefore, both the sandwich and PIP systems have higher critical buckling temperatures of 407.5°C and 547.1°C, respectively. Additionally, the low coefficient of thermal expansion in the core layer of the PIP system results in a higher critical buckling temperature compared to all other pipelines.

3.4 Subsea and buried conditions

The primary cause of buckling in subsea and buried pipelines is the longitudinal compressive force exerted on these structures due to temperature and pressure. When the temperature inside the subsea pipelines increases, the pipeline tends to expand. Since it rests on the seabed, this expansion is resisted by

Table 3 Constant for multilayer pipelines under subsea conditions

Types of pipelines	Single-walled	Liner	Sandwich	PIP
Constant (k)	2.20	2.30	3.33	3.37

the friction between the pipeline and the seabed. When the thermal expansion force exceeds this frictional resistance, the pipeline will buckle laterally. As shown in Fig. 12(a), it is clearly indicated that the perfect pipelines on a rigid seabed first undergo lateral buckling at low temperatures of 547°C, and subsequently buckle in the vertical direction at higher temperatures of 915°C. Therefore, the buckling mode of pipelines on an even seabed undergoes lateral buckling. The results of this numerical analysis agree well with the Hobbs (1984) analytical solution for perfect subsea pipelines.

The critical buckling load obtained from this numerical analysis is equal to 2.2 times the critical buckling load (P_c) of a clamped column under axial load. The Croll (1997) analysis indicated that the critical buckling load of the pipelines with imperfection is two times the critical load of the clamped column with axial load. Based on the simplified model of the Croll analysis, the critical buckling load for this numerical analysis is expressed in the following equation

$$(P_{cri})_{\text{pipeline}} \approx 2.2P_c = \frac{8.8\pi^2 EI}{L^2} \tag{9}$$

$$P_c = \frac{4\pi^2 EI}{L^2}$$

where P_c represents the critical buckling load of the clamped column under axial load.

The above equation can be written as follows

$$(P_{cri})_{\text{pipeline}} \approx kP_c \tag{10}$$

where k represents the constant. For the single-walled pipeline, the value of k is 2.20.

Similarly, the value of constant k for liner, sandwich, and PIP systems is listed in Table 3.

In the case of a constant temperature variation across the radius of the pipeline, the computed critical buckling temperature from this numerical analysis correlates well with that from the Martinet (1938) and Croll (1997) analyses. The critical buckling temperature determined from the present analysis for constant temperature variation is 547.23°C for a coefficient of friction of 0.4, whereas the Martinet and Croll analyses yielded values of 488.40°C and 496.66°C, respectively. This indicates that the critical buckling temperature obtained from this numerical analysis is 12% and 10% higher than their results

The critical buckling load from the Martinet and Croll analyses is given by the following expression

$$P = 3.962\left(\frac{EIq}{\tilde{w}}\right)^{1/2} \text{ and } P = 4.029\left(\frac{EIq}{\tilde{w}}\right)^{1/2} \tag{11}$$

where q and ^{w} represent the weight per unit length of the pipeline and the fixed displacement, respectively. Based on the expressions above, the critical buckling load for this analysis is given by

$$P = 4.437\left(\frac{EIq}{\tilde{w}}\right)^{1/2} \tag{12}$$

If the coefficient of friction between the seabed and the pipelines is increased from 0.4 to 0.6, the critical buckling temperature decreases from 547 °C to 519°C, as shown in Fig. 12(a). Consequently, the deviation of the buckling temperature is reduced from 12% to 6.26% and from 10% to 4.5% compared to the analyses by the Martinet and Croll, respectively.

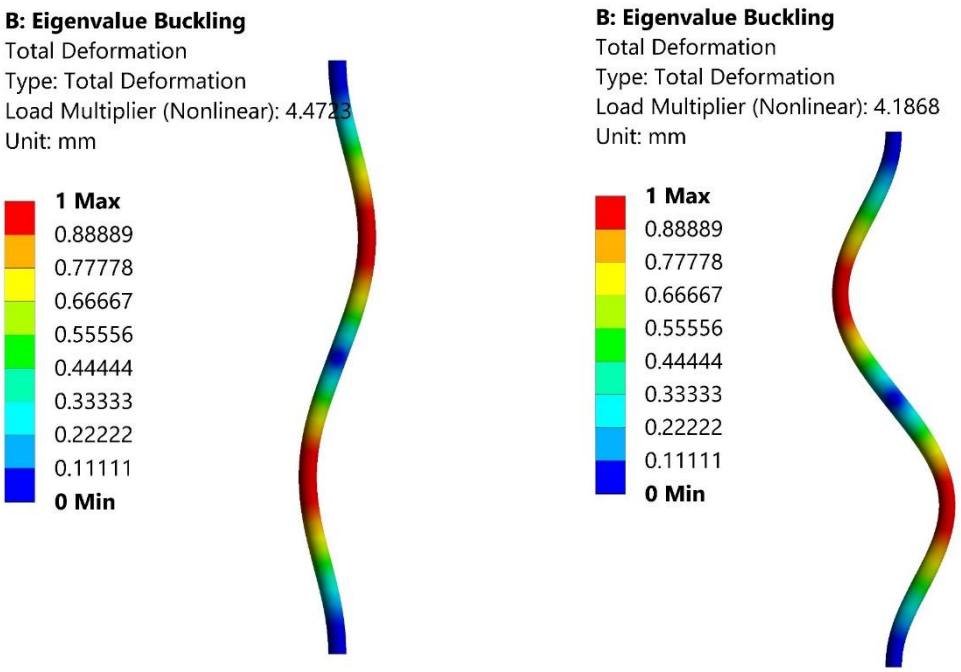

(i) μ = 0.4 (ii) μ = 0.6

(a) Lateral buckling mode

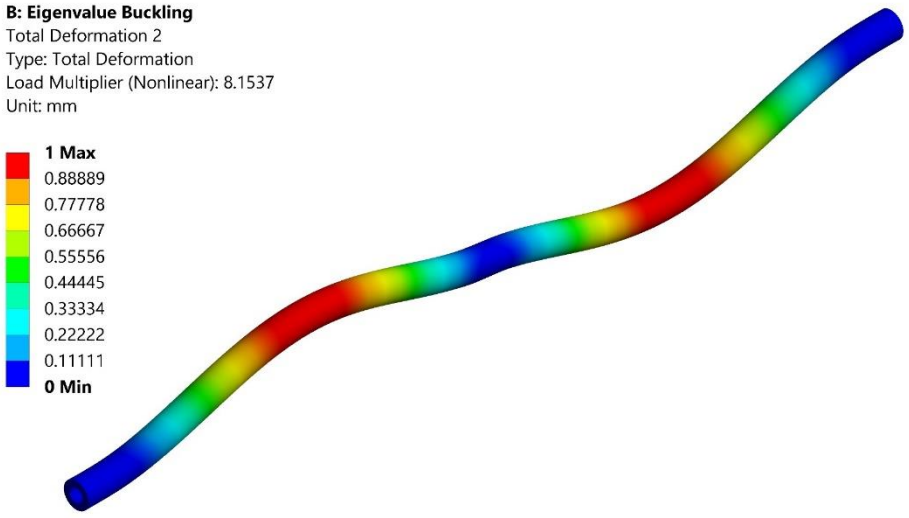

(b) Upheaval buckling mode

Fig. 12 Buckling modes of subsea pipeline

The upheaval mode of pipeline buckling under buried conditions is illustrated in Fig. 13 for an embedment depth of 0.5 m. Due to the applied temperature being above the ambient temperature, the pipeline starts to expand freely. However, because of the fixed end conditions, it cannot expand unrestrictedly. As a result, the pipeline will experience axial compressive forces. If the force that the

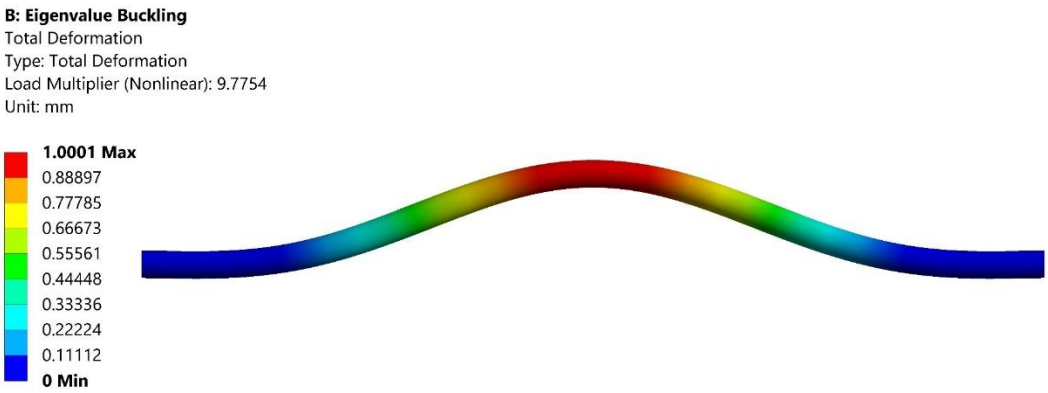

Fig. 13 Upheaval buckling in buried pipeline

pipeline exerts on the soil exceeds the vertical support provided by the pipe's weight, its bending stiffness, and the resistance of the soil above, the pipe may elevate, resulting in significant vertical movement that can lead to upheaval buckling in buried pipelines.

For embedment depths of 0.5 m, 0.75 m, and 1 m, the corresponding upheaval buckling temperatures are 589°C, 595°C, and 603°C respectively, indicating that significant temperature changes are required to induce upheaval buckling in buried pipelines with greater embedment depths. Therefore, the critical buckling temperature of upheaval buckling in buried pipelines increases with embedded depth or cover height, indicating that it depends on their embedded depth.

The effects of friction between the pipeline and the ground play a major role in the critical buckling temperature of buried pipelines, as they are fully covered with soil, unlike subsea pipelines. In contrast, seabed soil conditions have little impact on the critical buckling temperature of subsea pipelines. Generally, in a buried pipeline, uplift resistance is weaker than lateral resistance and resistance to downward buckling. As a result, global upheaval buckling is the primary buckling mode for buried pipelines.

The critical buckling temperature of pipelines under buried conditions, expressed in terms of a clamped column under axial load, is given by the following equation

$$(P_{cri})_{\text{pipeline}} \approx kP_c$$

The value of constant k for single-walled, liner, sandwich, and PIP systems for the buried conditions is listed in Table 4.

The buckling temperature of buried pipelines does not depend on the stiffness of the pipelines during thermal load, so there is no significant variation in the critical buckling temperature of these pipelines compared to subsea conditions. However, thermal buckling in buried pipelines depends on more parameters compared to subsea pipelines, such as soil properties, uplift resistance, and the height of soil cover or embedment depth.

The critical buckling temperature of all the aforementioned pipelines under subsea and buried conditions is illustrated in Fig. 14. The numerical findings indicate that the PIP system has a higher buckling resistance than all other pipelines, with critical buckling temperatures of 875°C and 682°C under subsea and buried conditions, respectively, due to the low coefficient of thermal expansion in the core layer of the PIP system.

Table 4 Constant for multilayer pipelines under buried conditions

Types of pipelines	Single-walled	Liner	Sandwich	PIP
Constant (k)	2.37	2.32	2.48	2.62

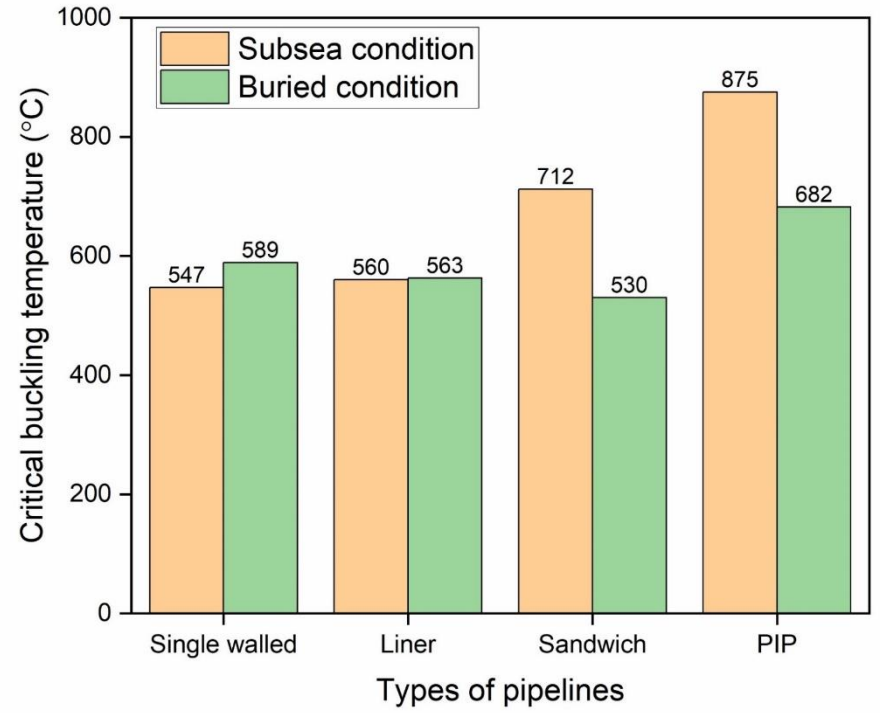

Fig. 14 Critical buckling temperature of pipelines under subsea and buried conditions

4. Conclusions

In this research, numerical simulations are employed to explore the thermal buckling analyses of various offshore pipeline types, namely single-walled pipeline, lined pipeline, sandwich pipeline, and pipe-in-pipe systems under subsea and buried conditions. The temperature and stress variations along the radius, as well as the total deformation of all pipelines, are presented. The numerically calculated critical buckling temperature of all the above-mentioned pipelines is compared to that of an equivalent single-walled pipeline. The current numerical study leads to the following conclusions:

- The maximum temperature obtained from the steady-state thermal analysis for equivalent single-walled and lined pipelines is 4.77°C and 4.83°C, respectively. These temperatures are approximately the same as the seawater temperature, which is lower than the wax appearance temperature. Therefore, insulation layers must be considered for offshore pipelines.
- The numerical findings indicate that the temperature variation along the inner and outer pipes of the sandwich and PIP system remains almost constant, while the temperature variation along the radius of the insulation layer decreases.

- The sandwich and pipe-in-pipe systems exhibit notable differences in their stress variation across the radius. In the sandwich pipeline, the outer pipe experiences the highest stress, whereas, in the PIP system, the inner pipe undergoes the maximum stress. However, the stress levels within the insulation layers are very small or negligible for both pipeline configurations.
- The lined pipeline's critical buckling temperature of 250.05°C, is almost identical to that of the equivalent single-walled pipeline under linear eigenvalue buckling analysis.
- The sandwich pipeline is experiencing maximum stress of 246.67 MPa, which is higher than that of all the other pipelines. Furthermore, it has a critical buckling temperature of 407.53°C.
- Compared to all other pipelines, the pipe-in-pipe system has the highest critical buckling temperature of 547.07°C, which is 34% higher than that of sandwich the pipeline and 116% higher than the equivalent single-walled pipeline.
- The thermal buckling analysis results show that lateral buckling occurs at low temperatures compared to upheaval buckling in pipelines laid on the seabed or under subsea conditions.
- The embedment depth of the buried pipeline significantly influences the critical buckling temperature in upheaval buckling under buried conditions.
- As a result, the insulation material greatly influences the critical buckling temperature of the pipelines.

Acknowledgments

We are very grateful to the funding agency, AR & DB, Ministry of Defence, file number ARDB/01/2031964/M/I for providing financial assistance for conducting our research work.

References

Abyanifor, M. and Bahaari, M.R. (2021), "A new approach for finite element-based reliability evaluation of offshore corroded pipelines", *Int. J. Press. Ves. Pip.*, **193**, 104449. https://doi.org/10.1016/j.ijpvp.2021.104449.

ANSYS 19.0 Release, ANSYS, Inc., 275 Technology Drive, Canonsburg, PA 15317.

Barletta, A., Lazzari, S., Zanchini, E. and Terenzi, A. (2008), "Transient heat transfer from an offshore buried pipeline during Start-up Working Conditions", *Heat Transfer Eng.*, **29**(11), 942-949. https://doi.org/10.1080/01457630802186031.

Bell, E., Lu, Y., Daraboina, N. and Sarica, C. (2021), "Thermal methods in flow assurance: A review", *J. Nat. Gas Sci. Eng.*, **88**, 103798. https://doi.org/10.1016/j.jngse.2021.103798.

Bhardwaj, U., Teixeira, A.P. and Soares, C.G. (2022), "Probabilistic collapse design and safety assessment of sandwich pipelines", *J. Mar. Sci. Eng.*, **10**(10), 1435. https: doi.org/10.3390/jmse10101435.

Cai, J., Le Grognec, P. and Nême, A. (2023), "Analytical and numerical study of the lateral buckling of an imperfect pipe accounting for torsional effects", *Ocean Eng.*, **271**, 113686. https://doi.org/10.1016/j.oceaneng.2023.113686.

Cai, J. and Le Grognec, P. (2022), "Lateral buckling of submarine pipelines under high temperature and high pressure - A literature review", *Ocean Eng.*, **244**, 110254. https://doi.org/10.1016/j.oceaneng.2021.110254.

Castello, X. and Estefen, S.F. (2008), "Sandwich pipes for ultra-deep-water applications", *Proceedings of the Offshore Technology Conference*, May 5th-8th, OTC-19704-MS, Texas, U.S.A. https://doi.org/10.4043/19704-MS.

Chen, Z., Yi, Y.B., Bao, K. and Zhao, J. (2019), "Numerical analysis of the coupling between frictionally excited thermoelastic instability and thermal buckling in automotive clutches", *Proc IMechE Part J: J Eng. Tribology*, **233**(1), 178-187. https://doi.org/10.1177/1350650118772664.

Cheng, X., Bo, Y., Zhengwei, Z., Jinjun, Z., Jinjia, W. and Shuyu, S. (2010), **"**Numerical simulation of a buried hot crude oil pipeline during shutdown", *Pet. Sci.*, **7**(1), 73-82. https://doi.org/10.1007/s12182-010-0008-x.

Croll, J.G.A. (1998), "A simplified model of upheaval thermal buckling of subsea pipelines", *Thin-Walled Struct.*, **29**(1-4), 59-78. https://doi.org/10.1016/S0263-8231(97)00036-0.

Escobedo, J.J.B., Nieckele, A.O. and Azevedo, L.F.A. (2005), "Transient thermal analysis in subsea pipelines", *Proceedings of the 18th International Congress of Mechanical Engineering*, COBEM, November 6th -11th, Brazil.

Guo, Y., Chen, X. and Wang, D. (2016), "Analytical and numerical analysis for unbonded flexible risers under axisymmetric loads", *Ocean Syst. Eng.*, **6**(2), 129-141. httpa://doi.org/10.12989/ose.2016.6.2.129.

Guo, L.P., Run, L. and Yan, S.W. (2013), "Global buckling behaviour of submarine unburied pipelines under thermal stress", *J. Cent. South Univ.*, **20**, 2054-2065. httpa://doi.org/10.1007/s11771-013-1707-4.

Guo, B. (2005), **"**Analytical solutions for steady and transient temperatures in oil pipelines", *Petroleum Sci. Tech.*, **23**, 307-325. https://doi.org/10.1081/LFT-200028301.

Hobbs, R.E. (1984), "In-service buckling of heated pipelines", *J. Transp. Eng.*, **110**(2), 175-189. https://doi.org/10.1061/ (ASCE)0733-947X(1984)110:2(175).

Holman, J.P. (2010), Heat Transfer, McGraw-Hill, New York.

Ismail, S., Sadek, S., Najjar, S.S. and Mabsout, M. (2021), "Numerical finite element modelling of soil resistance against upheaval buckling of buried submarine pipelines", *Appl. Ocean Res.*, **106**, 102478. https://doi.org/10.1016/j.apor.2020.102478.

Karar, O., Emani, S., Gounder, R.M., Thant, M.M.M., Mukhtar, H., Sharifpur, M. and Sadeghzadeh, M. (2021), "Experimental and numerical investigation on convective heat transfer in actively heated bundle-pipe", *Eng. Appl. Comput. Fluid Mech.*, **15**(1), 848-864. https://doi.org/10.1080/19942060.2021.1920466.

Kyriakides, S. (2002), "Buckle propagation in pipe-in-pipe systems. Part I Experiments", *Int. J. Solids Struct.*, **39**(2), 351-366. https://doi.org/10.1016/S0020-7683(01)00163-9.

Li, Z., Hu, D., Shen, M., Huang, H. and Ou, Z. (2024), "Thermal upheaval buckling framework of a graphene-reinforced subsea pipeline laid on an arched concave seabed", *Eng. Struct.*, **318**, 118750. https://doi.org/10.1016/j.engstruct.2024.118750.

Li, C., Liu, R., Wang, X. and Hao, H. (2021), "Experimental and theoretical studies on lateral buckling of submarine pipelines", *Mar. Struct.*, **78**, 102983. https://doi.org/10.1016/j.marstruc.2021.102983.

Liu, Y. (2011), "Thermal buckling of metal oil tanks subject to an adjacent fire", Ph.D. Thesis, University of Edinburgh, Scotland, U.K.

Moghaddam, A.S., Mohammadnia, S. and Sagharichiha, M. (2015), "Analysis of offshore pipeline laid on 3D seabed configuration by Abaqus", *Ocean Syst. Eng.*, **5**(1), 31-40. https://doi.org/10.12989/ose.2015.5.1.031.

Mondal, B.C. and Dhar, A.S. (2017), "Upheaval buckling of surface-laid offshore pipeline", *Appl. Ocean Res.*, **66**, 146-155. https://doi.org/10.1016/j.apor.2017.05.012.

Rajeev, P. and Robert, D.J. (2017), "Effect of irregular seabed profile on upheaval buckling of buried offshore pipelines", *J. Pip. Syst. Eng. Pract.*, **8**(4), https://doi.org/10.1061/(ASCE)PS.1949-1204.0000281.

Subedi, R., Hawlader, B., Roy, K. and Dhar, A. (2024), "Numerical modelling of upheaval buckling of offshore pipelines with unstressed and stressed initial imperfections", *Ocean Eng.*, **310**, 118781. https://doi.org/10.1016/j.oceaneng.2024.118781.

Vazouras, P., Tsatsis, M. and Dakoulas, P. (2021), "Thermal upheaval buckling of buried pipelines: Experimental behavior and numerical modelling", *J. Pip. Syst. Eng. Pract.*, **12**(1), 04020057. https://doi.org/10.1061/(ASCE)PS.1949-1204.0000507.

Vishnuvardhan, S., Murthy, A.R. and Choudhary, A. (2023), "A review on pipeline failures, defects in pipelines and their assessment and fatigue life prediction methods", *Int. J. Press. Ves. Pip.*, **201**, 104853. https://doi.org/10.1016/j.ijpvp.2022.104853.

Wang, Y., Wei, N., Wan, D., Wang, S. and Yuan, Z. (2019), "Numerical simulation for preheating new submarine hot oil pipelines", *Energies*, **12**(18), 3518. https://doi.org/10.3390/en12183518.

Wang, Z., Tang, Y. and Soares, C.G. (2021), "Analytical and numerical study on lateral buckling of imperfect subsea pipelines with nonlinear lateral pipe-soil interaction model", *Ocean Eng.*, **221**, 108495. https://doi.org/10.1016/j.oceaneng.2020.108495.

Wang, Z., Chen, B. and Soares, C.G. (2022), "Analytical study on the upheaval thermal buckling of sandwich pipes", *Mar. Struct.*, **85**, 103245. https://doi.org/10.1016/j.marstruc.2022.103245.

Wang, Z., Chen, Z., He, Y. and Liu, H. (2017), "Numerical study on lateral buckling of fully bonded sandwich pipes", *Int. J. Steel Struct.*, **17**(3), 863-875. https://doi.org/10.1007/s13296-017-9002-0.

Wang, Z., Huachen, Z., Liu, H. and Bu. Y. (2015), "Static and dynamic analysis on upheaval buckling of unburied subsea pipelines", *Ocean Eng.*, **104**, 249-256. https://doi.org/10.1016/j.oceaneng.2015.05.019.

Wang, Z. and Soares, C.G. (2022), "Theoretical investigation on the upheaval thermal buckling of a lined subsea pipeline", *Ocean Eng.*, **261**, 111843. https://doi.org/10.1016/j.oceaneng.2022.111843.

Wang, Z., Li, S., Xu, Q. and He, F. (2023), "Lateral buckling of subsea pipelines triggered by combined sleeper and distributed buoyancy section", *Mar. Struct.*, **88**, 103343. https://doi.org/10.1016/j.marstruc.2022.103343.

Wang, H., Wang, Z., Lei, Z., Guo, Z., Liu, D. and Wang, K. (2024), "Pipeline lateral buckling triggered by the residual curvature with tri-linear axial pipe-soil interaction", *Appl. Ocean Res.*, **151**, 104148. https://doi.org/10.1016/j.apor.2024.104148.

Yang, Y., Wan, F., Guan, F., Tian, H. and Chen, W. (2024), "Buckling behavior of sandwich pipe under external pressure and lateral load", *Int. J. Press. Ves. Pip.*, **207**, 105114. https://doi.org/10.1016/j.ijpvp.2023.105114.

Yuan, L. and Kyriakides. (2014), "Liner wrinkling and collapse of bi-material pipe under bending", *Int. J. Solids Struct.*, **51**, 599-611. https://doi.org/10.1016/j.ijsolstr.2013.10.026.

Zechao, Z., Jinghai, Y., Zhihua, C., Jinchao, H., Zhe, W. and Hongbo, L. (2020), "Experimental study on the buckling of subsea pipe-in-pipe systems", *J. Test. Eval.*, **48**(1), 409-427. https://doi.org/10.1520/JTE20180595.

Zhang, X. and Duan, M. (2015), "Prediction of the upheaval buckling critical force for imperfect submarine pipelines", *Ocean Eng.*, **109**, 330-343. https://doi.org/10.1016/j.oceaneng.2015.09.022.

Zhang, X., Duan, M., Wang, Y. and Li, P. (2016), "Parameters study on lateral buckling of submarine PIP pipelines", *Ocean Syst. Eng.*, **6**(1), 99-115. https://doi.org/10.12989/ose.2016.6.1.099

PS